JOURNAL OF PROPULSION AND POWER
Vol. 19, No. 1, January–February 2003

Technical Notes

TECHNICAL NOTES are short manuscripts describing new developments or important results of a preliminary nature. These Notes cannot exceed 6 manuscript pages and 3 figures; a page of text may be substituted for a figure and vice versa. After informal review by the editors, they may be published within a few months of the date of receipt. Style requirements are the same as for regular contributions (see inside back cover).

Optimal Actuator/Sensor Placement for Control of Combustion Instabilities

Nidal Al-Masoud* and Tarunraj Singh†
State University of New York at Buffalo,
Buffalo, New York 14260

I. Introduction

THE problem of choosing the appropriate number and locations of actuators and sensors is an important part in the design of any control system. The efficiency and performance of any control law is greatly affected by the placement of the actuators and sensors. Thus, there is a need for a technique that is capable of determining the optimal set of locations and, consequently, the minimal number of actuators.

Several quantitative measures have been developed for the purpose of selecting actuator locations to control structural systems.[1−5] These methods are extended for optimal actuator placement to control thermoacoustic instabilities. The analysis is based on the concepts of the degree of controllability and component cost, which are explained later in this Note.

II. Theoretical Combustion Model

In this section, a theoretical model for a two-phase flow in a liquid-fueled propulsion system is presented. The final form of the conservation equations are[6]

$$\frac{\partial \rho}{\partial t} + \nabla \cdot (\rho \boldsymbol{u}_g) = \mathcal{W} \tag{1}$$

$$\rho \frac{\partial \boldsymbol{u}_g}{\partial t} + \rho \boldsymbol{u}_g \cdot \nabla \boldsymbol{u}_g + \nabla p = \boldsymbol{\mathcal{F}} \tag{2}$$

$$\frac{\partial p}{\partial t} + \boldsymbol{u}_g \cdot \nabla p + \bar{\gamma} p \nabla \cdot \boldsymbol{u}_g = \mathcal{P} \tag{3}$$

The source terms in these equations represent the exchange of mass, momentum, and energy between liquid and gas medium in the chamber. The governing wave equation is derived by expressing all dependent variables in Eqs. (1–3) as the sum of mean and fluctuating components[6,7]:

$$\nabla^2 p' - \frac{1}{\bar{a}^2}\frac{\partial^2 p'}{\partial t^2} = h + h_c \tag{4}$$

$$\boldsymbol{n} \cdot \nabla p\prime = -(\boldsymbol{f} + \boldsymbol{f}_c) \tag{5}$$

where p' is the pressure fluctuation and $\bar{a}$ is the average speed of sound in the chamber. Quantities h and $\boldsymbol{f}$ accommodate the influences of mean flow, combustion, and acoustic motions. Terms h_c and $\boldsymbol{f}_c$ represent the effects of external control input.

If the source terms in Eqs. (4) and (5) are treated as a small perturbations of classical acoustics, the solution can be approximated as a synthesis of normal modes ψ_n, with time-varying amplitude η_n, and the unsteady pressure is given by[6,7]

$$p'(\boldsymbol{r}, t) = \bar{p} \sum_{n=1}^{\infty} \eta_n(t)\psi_n(\boldsymbol{r}) \tag{6}$$

where the normal mode shape ψ_n satisfies the classical acoustic wave equation. For pure longitudinal oscillations in a uniform cylindrical chamber, the mode shape is given by $\psi_n = \cos(n\pi x/L)$. When the Galerkin method is used, Eqs. (4) and (5) are replaced by an equivalent set of ordinary differential equations that describe the amplitude of the pressure oscillation. The linear representation of the system dynamics is[6]

$$\ddot{\eta}_n(t) + \omega_n^2 \eta_n(t) + \sum_{i=1}^{n} [D_{ni}\dot{\eta}_i(t) + E_{ni}\eta_i(t)] = U_n(t) \qquad n = 1, 2, \ldots, n \tag{7}$$

where D_{ni} and E_{ni} are linear coefficients associated with growth rate and frequency shift of each mode[6] and U_n is the control input. When it is assumed that the unsteady pressure field is monitored by ℓ point sensors each at the position x_j, then the measurement is given by[6]

$$y_j(t) = \bar{p} \sum_{i=1}^{n} \eta_i(t)\psi_i(x_j), \qquad j = 1, \ldots, \ell \tag{8}$$

In state-space representation, Eqs. (7) and (8) are given by

$$\dot{x}(t) = A_{n\times n}x(t) + B_{n\times m}u(t), \qquad y(t) = C_{\ell\times n}x(t) \tag{9}$$

where n, m, and ℓ are number of states, inputs, and outputs, respectively.

III. Optimal Actuator/Sensor Placement Algorithm

The concept of controllability is closely related to the existence of a feasible control law that makes the closed-loop system stable with respect to a desired state or trajectory. Several algorithms are available to test the systems controllability[2]; however, from these tests, one can only arrive at a binary (yes/no) answer: It does not state how controllable the system is.

As an improvement over the binary controllability tests, Hamdan and Nayfeh[2] proposed two quantitative measures that provide information of how controllable each mode is. Those measures make use of the angle between the left eigenvectors of the system matrix A and the columns of the control influence matrix B as shown in Fig. 1.

Received 27 October 2001; revision received 2 January 2002; accepted for publication 5 September 2002.

*Ph.D. Candidate, Department of Mechanical and Aerospace Engineering. Member AIAA.

†Associate Professor, Department of Mechanical and Aerospace Engineering. Member AIAA.

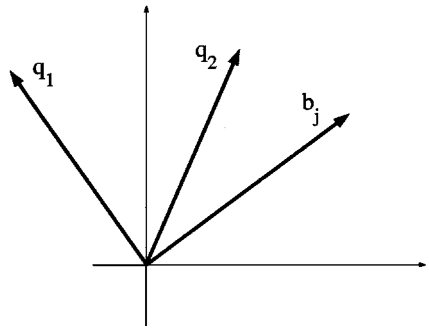

Fig. 1 Hamdan and Nayfeh approach.[2]

The first measure is defined as

$$\cos\theta_{ij} = \frac{\left|\boldsymbol{q}_i^T \boldsymbol{b}_j\right|}{\|\boldsymbol{q}_i\|\,\|\boldsymbol{b}_j\|} \tag{10}$$

where $\boldsymbol{q}_i'$ are the eigenvectors of the system matrix A satisfying $A^T\boldsymbol{q}_i = \lambda_i \boldsymbol{q}_i$, with λ_i being the ith eigenvalue of A. The angle θ_{ij} is a measure of the controllability of the ith mode from the jth actuator input and is taken to be acute. As θ_{ij} approaches 90 deg, the influence of the jth on the ith mode diminishes.

Using this preposition, we can calculate a $n \times m$ matrix of measures of controllability, whose ijth element is computed using Eq. (10). This matrix is designated as $\cos(\Theta)$. To account for the different power levels from different inputs on each mode controllability, Hamdan and Nayfeh[2] defined the following $m \times m$ diagonal matrix D:

$$D = \mathrm{diag}[\|\boldsymbol{b}_1\|, \|\boldsymbol{b}_1\|, \ldots, \|\boldsymbol{b}_m\|] \tag{11}$$

Define $\boldsymbol{f}_i$ as the ith row of $F_{n\times m} = (\cos\Theta)D$. The Euclidean norm of the vector $\boldsymbol{f}_i$ is defined as the gross measure of controllability ρ_i given by

$$\rho_i = \|\boldsymbol{f}_i\|$$

$$\text{where} \quad \boldsymbol{f}_i^T = [\cos\theta_{i1}\|\boldsymbol{b}_1\| \quad \cos\theta_{i2}\|\boldsymbol{b}_2\| \quad \ldots \quad \cos\theta_{im}\|\boldsymbol{b}_m\|] \tag{12}$$

Each entry of the vector $\boldsymbol{f}_i$ is the length of the component of a column vector of B in the direction of $\boldsymbol{q}_i$. The effective power in controlling the ith mode depends on the component of the vector $\boldsymbol{b}_j$ in the direction of $\boldsymbol{q}_i$. If the latter component is zero, then the jth input does not inject any power into the ith mode.

IV. Component Cost and Performance Measures

The component cost can be defined as the fraction of the system performance metric V due to the participation of each state variables. The contribution of each mode or physical state variable to the cost function can be used as a measure of the relative importance of that state. The cost function V and the contribution V_{x_i} of the state variable x_i can be computed as follows[1,3]:

$$V_{xi} = \left[XC_d^T Q_v C_d\right]_{ii}, \qquad V = \mathrm{tr}\left[Q_v C_d X C_d^T\right], \qquad V = \sum V_{xi} \tag{13}$$

where C_d and Q_v are output matrix and weighting matrix, respectively, and X is defined as the controllability gramian that satisfies the Lyapunov equation (see Ref. 3)

$$XA^T + AX + BB^T = 0 \tag{14}$$

Motivated by the concepts of degree of controllability and the component and modal costs presented, the weighted measure of controllability α is

$$\alpha = \sum_{i=1}^{n} \frac{V_i}{V}\rho_i^2 \tag{15}$$

where ρ_i is defined in Eq. (12).

We consider a variety of objective functions to determine the optimal location of the actuators based on the linear combustion model. These objective functions are based mainly on the concepts of degree of controllability and component cost just discussed. These concepts are also used to modify some previously reported performance measures.

Because the system is not stable, it is necessary to find a stabilizing state feedback gain matrix $\mathcal{K}$. This matrix is not unique; its choice depends on the desired system response. The reciprocal of the norm of the gain matrix $\mathcal{K}$ needed to place the system poles at the desired location vs the actuator location is shown in Fig. 2, which can be used as a criterion for selecting the actuator location.

The most effective position of single input/single output (SISO) arrangement is the head/end position, where the gain is minimum. The spikes on the curves correspond to points where certain mode is uncontrollable, which theoretically means an infinite gain is needed to stabilize that particular mode; therefore, these locations should be avoided. In terms of Eq. (10), these infinite gain points correspond to the points at which θ is closed to 90 deg.

In the rest of this Note, we will be studying a variety of cost functions to determine the relationship between the optimal actuator location and the power consumed.

The total cost function V defined in Eq. (13) with Q_v set to unity is the first cost function considered:

$$\max J_1 = V = \mathrm{tr}\left[C_d X C_d^T\right] \tag{16}$$

The performance index J_1 to be maximized is shown by the solid line in Fig. 3. Higher costs are associated with the lower stabilizing

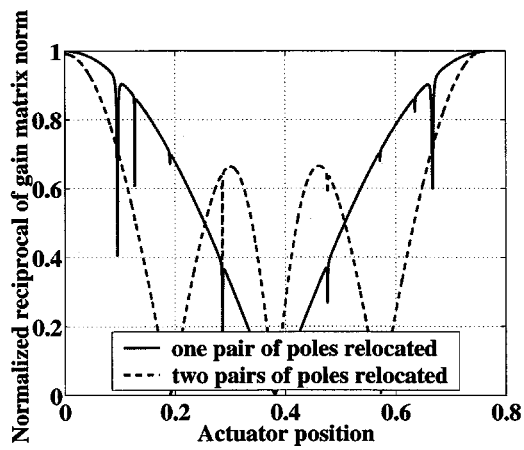

Fig. 2 Reciprocal of the gain matrix.

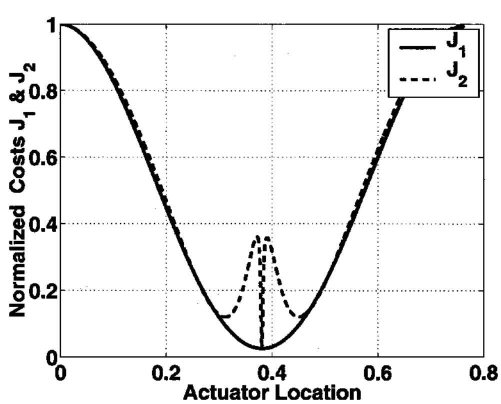

Fig. 3 J_1 and J_2 costs.

gain, as shown in Fig. 2; thus, the optimal location is where the stabilizing gain is minimum, which is the head or the end of the combustor.

The weighted gross measure of controllability defined in Eq. (15) denoted hereafter by J_2 is given by

$$\max J_2 = \sum_{i=1}^{\infty} \frac{V_i}{V} \rho_i^2 \tag{17}$$

This metric is shown by the dashed line in Fig. 3. The optimal location is at the head or the end of the combustor, using the same argument of cost J_1.

Consider the following two measures:

$$\max J_3 = \sum_{i=1}^{N} \frac{\left|q_i^T b_j\right|}{\|q_i\|\|b_j\|} + \sum_{i=N+1}^{\infty} \frac{\|q_i\|\|b_j\|}{\left|q_i^T b_j\right|} \tag{18}$$

$$\max J_4 = \sum_{i=1}^{N} \frac{V_{xi}}{V} \frac{\left|q_i^T b_j\right|}{\|q_i\|\|b_j\|} + \sum_{i=N+1}^{\infty} \frac{V_{xi}}{V} \frac{\|q_i\|\|bj\|}{\left|q_i^T b_j\right|} \tag{19}$$

where N is number of the controlled modes. The performance index J_3 maximizes the sum of the controllability measures of the controlled modes, while at the same time minimizes the sum associated with the residual modes. The controllability measures are the entries of the vector $\boldsymbol{f}_i$ defined in Eq. (12). The cost function J_4 is a weighted form of index J_3. The component cost serves as the weighting factor for the elements of J_3. Figure 4 illustrates the siginificant difference between the unweighted metric J_3 (dashed line) and weighted metric J_4 (solid line). When the control power is compared for the unweighted and weighted metrics, a considerable improvement is noticed when the contribution of each mode is considered as shown in Table 1.

To further investigate the effect of component weighting, two previously reported measures are considered. The first measure is due to Fung et al.[7] and the proposed modifications using component cost are given by

$$\min J_5 = W_N \left(\sum_{n=1}^{N} [1 - |\psi_n(x_a)|]^2 + W_R \sum_{i=N+1}^{\infty} [\psi_n(x_a)]^2 \right. \tag{20}$$

$$\min J_6 = \sum_{n=1}^{N} [1 - |\psi_n(x_a)|]^2 \frac{V_{xn}}{V} + \sum_{n=N+1}^{\infty} [\psi_n(x_a)]^2 \frac{V_{xn}}{V} \tag{21}$$

where W_N and W_R are weighting factors for modeled and residual modes. Note that a single factor W_N is associated with all modeled modes and W_R for all residual. The proposed modification associates a specific weight for each mode. The second index J_7 is due to Choe and Baruh,[8] and its proposed modification J_8 is

$$\min J_7 = \sum_{n=1}^{N} \left[1 \Bigg/ \left(\sum_{i=1}^{m} |B_{ri}| \right) \right] + \sum_{n=N+1}^{\infty} \left[\left(\sum_{i=1}^{\infty} |B_{ri}| \right) \Bigg/ (N+1) \right] \tag{22}$$

$$\min J_8 = \sum_{n=1}^{N} \left[1 \Bigg/ \left(\sum_{i=1}^{m} |B_{ri}| \frac{V_{xn}}{V} \right) \right] + \sum_{n=N+1}^{\infty} \left[\left(\sum_{i=1}^{\infty} |B_{ri}| \frac{V_{xn}}{V} \right) \Bigg/ (N+1) \right] \tag{23}$$

Figures 5 and 6 show the plots of the original cost function in dashed lines and the proposed modified versions of these costs.

Table 1 SISO actuator/sensor optimal location

	Noncollocated, $x_s = L/7.5$		Collocated, $x_s = x_a$	
Cost function	x_a	Normalized control power	x_a	Normalized control power
J_1	Head/end	1.00	Head/end	1.00
J_2	Head/end	1.00	Head/end	1.00
J_3	0.2864	2.6401	0.2864	2.6398
J_4	0.1125	1.1184	0.1176	1.1305
J_5	0.1007	1.0930	0.1007	1.0929
J_6	0.7407	1.0072	0.0553	1.0265
J_7	0.6641	1.0902	0.6641	1.0902
J_8	0.6769	1.0682	0.6385	1.1476

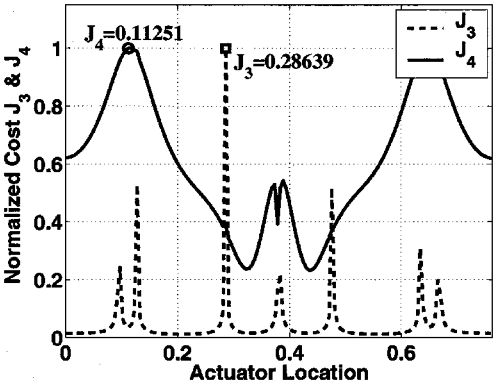

Fig. 4 J_3 **and** J_4 **costs.**

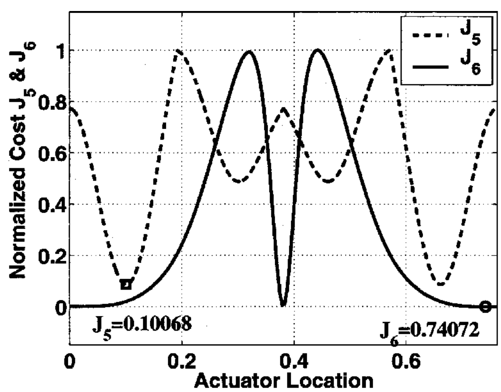

Fig. 5 J_5 **and** J_6 **costs.**

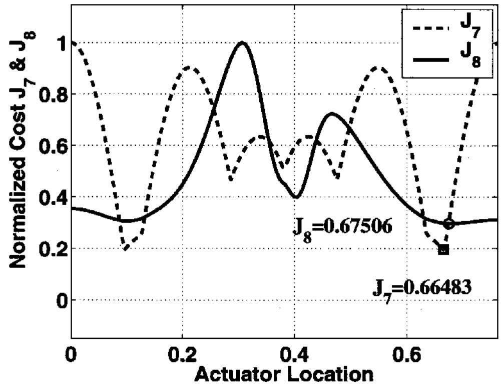

Fig. 6 J_7 **and** J_8 **costs.**

Table 1 is a tabulation of the optimal location of the actuator for the noncollocated and collocated cases. Because all of the controllers were designed to generate identical dynamics, the control power is used as a corroborator of the use of the weighted cost functions for determining the optimal location of the actuator. Table 1 lists the optimal locations of the actuators and the normalized control power. It can be seen that weighting the cost function with the component cost results in a significant reduction of the control power as in J_3 and J_4, J_5 and J_6, and J_7 and J_8. Note that J_1, J_2, J_6, and J_8 result in requiring nearly identical control power.

V. Conclusions

In this Note, a methodology for determining the optimal actuator and sensor locations for the control of combustion instabilities is presented. The approach relies on the quantitative measures of the degree of controllability and component cost. These criteria are arrived at by considering the energies of system's inputs and outputs. The optimality criteria for sensor and actuator locations provide a balance between the importance of the lower-order (controlled) and the higher- (residual) order modes.

In previous studies, the cost has been a function of the control influence matrix only and the relative contribution of the modes to the output has not been considered. This Note describes a systematic procedure that associates weights that reflect the importance of each state variable or mode in a given cost function, thus, increasing the system controllability and its overall performance. The procedure can be extended to optimize the number of actuators in multi-input applications by removing the least effective actuators, one at a time. In addition, it can be applied to a discrete set of candidate locations. The control energy level can be taken as a factor in the selection process, in a sense that if the head/end location is not practical, the optimal location can be moved to the next control energy level and so on. In general, the optimal locations are found to be at locations where the lower modes have the greatest contribution and the higher modes are minimally represented in the cost functions. Physically speaking, at these locations, the lower modes are the most controllable because the point of application of the actuation power is far from the nodal point of these modes, which means the required control is small and the higher modes are not excited.

References

[1]Skelton, R., and Yousuff, A., "Component Cost Analysis of Large Scale Systems," *International Journal of Control*, Vol. 137, No. 2, 1983, pp. 285–304.

[2]Hamdan, A., and Nayfeh, A., "Measure of Modal Controllability and Observability for First- and Second-Order Linear Systems," *Journal of Guidance, Control, and Dynamics*, Vol. 12, No. 5, 1989, pp. 421–428.

[3]Junkins, J., and Kim, Y., *Introduction to Dynamics and Control of Flexible Structures*, AIAA, Washington, DC, 1993.

[4]Longman, R. W., and Alfriend, K. T., "Energy Optimal Degree of Controllability and Observability for Regulator and Maneuver Problems," *Journal of the Astronautical Sciences*, Vol. 38, 1990, pp. 87–103.

[5]Lim, K., "Method for Optimal Actuator and Sensor Placement for Large Flexible Structure," *Journal of Guidance, Control, and Dynamics*, Vol. 15, No. 1, 1992, pp. 49–57.

[6]Fung, Y.-T., Yang, V., and Sinha, A., "Active Control of Combustion of Instabilities with Distributed Actuators," *Combustion Science and Technology*, Vol. 78, 1991, pp. 217–245.

[7]Fung, Y.-T., Yang, V., and Sinha, A., "State-Feedback Control of Longitudinal Combustion Instabilities," *Journal of Propulsion and Power*, Vol. 8, No. 1, 1992, pp. 66–75.

[8]Choe, K., and Baruh, H., "Actuator Placement in Structural Control," *Journal of Guidance, Control, and Dynamics*, Vol. 15, No. 1, 1992, pp. 40–48.

Modified Mixing Analogy for Studies of Mixing in Supersonic Flows

Sadatake Tomioka*
National Aerospace Laboratory of Japan, Kakuda, Miyagi 981-1525, Japan
and
Lance S. Jacobsen† and Joseph A. Schetz‡
Virginia Polytechnic Institute and State University, Blacksburg, Virginia 24061-0203

Nomenclature

M = Mach number
P, p = total and static pressure
q = dynamic pressure
T = total temperature
V = velocity
α = injectant mass fraction
α_{mix} = injectant mass fraction deduced with modified mixing analogy, Eq. (3)
α^*_{mix} = injectant mass fraction deduced with original mixing analogy, Eq. (1)
β = enthalpy deficit factor due to induced vorticity
ρ = density

Subscripts

a = freestream
c = unheated injection
h = heated injection
j = injectant
p = measured with in-stream probe

Introduction

MIXING augmentation techniques[1–4] are an essential requirement for the development of the supersonic combustion ramjet (scramjet) engine. In recent works,[3,5] a high-molecular-weight injectant was utilized because hydrocarbon fuels became of greater interest.[6–8] However, many injectant concentration detection techniques depend mainly on the difference between the injectant molecular weight and that of the main flow so that their sensitivity is not sufficient compared to cases with lighter molecules, for example, helium, injected into air. In some previous work,[3] therefore, heated air was injected into an unheated supersonic crossflow, and the corresponding equivalent injectant concentration was deduced from the total temperature measurements and a mixing analogy as

$$\alpha^*_{\mathrm{mix}} = (T_p - T_a)/(T_j - T_a) \tag{1}$$

Received 30 March 2001; revision received 20 May 2002; accepted for publication 12 September 2002.

*Senior Researcher, Ramjet Propulsion Center, Kakuda Space Propulsion Laboratory. Member AIAA.

†Graduate Assistant, Aerospace and Ocean Engineering Department; currently, Postdoctoral Research Engineer, U.S. Air Force Research Laboratory, Dayton, OH 45433-7251. Member AIAA.

‡Fred D. Durham Chair, Aerospace and Ocean Engineering Department. Fellow AIAA.